Pers Ubiquit Comput (2007) 11:417–428
DOI 10.1007/s00779-006-0097-0

ORIGINAL ARTICLE

LuxTrace: indoor positioning using building illumination

Julian Randall · Oliver Amft · Jürgen Bohn · Martin Burri

Received: 11 August 2005 / Accepted: 9 November 2005 / Published online: 14 March 2007

Abstract Tracking location is challenging due to the numerous constraints of practical systems including, but not limited to global cost, device volume and weight, scalability and accuracy; these constraints are typically more severe for systems that should be wearable and used indoors. We investigate the use of wearable solar cells to track changing light conditions (a concept that we named LuxTrace) as a source of user displacement and activity data. We evaluate constraints of this approach and present results from an experimental validation of displacement and activity estimation. The results indicate that a distance estimation accuracy of 21 cm (80% quantile) can be achieved. A simple method to combine LuxTrace with complementary absolute location estimation methods is also presented. We apply carpet-like distributed RFID tags to demonstrate online learning of new lighting environments.

J. Randall (✉) · O. Amft · M. Burri
Wearable Computing Lab, ETH Zürich, Switzerland
e-mail: jfrandall@ieee.org
URL: www.wearable.ethz.ch

O. Amft
e-mail: amft@ife.ee.ethz.ch

M. Burri
e-mail: burrima@ee.ethz.ch

J. Bohn
Institute for Pervasive Computing, ETH Zürich, Switzerland
e-mail: bohn@inf.ethz.ch

1 Introduction

The LuxTrace project investigates the opportunities for using solar cells to simultaneously collect energy and track light level. As light conditions are location dependent, this radiance data can be used as context information to support the position tracking of a user indoors.

Advantages of extracting context data from indoor lights are that this infrastructure may be used without modification (i.e. the technology is minimally invasive) and this source of context data is generally untapped. Solar cells as sensors for wearable computing are attractive firstly as their low number of ''pixels'' (e.g. 1) implies that limited processing power may be sufficient. Secondly, as solar cells can be produced in thin (<1 m) low weight layers on a flexible substrate in a number of colours they better match garment specifications than other sensing devices. A third benefit of solar cells is that they can be used as a sensor and an energy harvesting device, thus contributing to the restricted energy available on the body.

The limitations of existing technologies are related to a number of factors including coverage, cost and location estimation accuracy. Satellite navigation for indoor application is unsatisfactory in all three categories given that it is generally not available indoors, is relatively expensive and the error of global positioning system (GPS) for example is of the order of 15–20 m [1]. This error can be reduced to 1–2 m by error correction using European Geostationary Navigation Overlay Service [2]. The European Galileo [3] system, planned to be commercially available by 2008, targets a global accuracy on the horizontal plane of up to 4 m for safety of life services and mass market applications, and up to 1 m for commercial applications. Galileo may offer horizontal accuracy in the centimetre-range by means of locally

augmented signals [4]. Numerous other location tracking technologies exist that provide *absolute position* estimations, e.g. radio frequency identification (RFID) tags [5] or wireless communication systems [6, 7]. Generally these technologies rely on supporting infrastructure. *Relative position* technologies include ultrasound [8] and inertial sensors, e.g. [9]. These systems suffer from continuous drift since no re-calibration mechanism is integrated. Some of these technologies have been developed in badge form, but generally have not been fully integrated into clothing.

Our investigations evaluate the potential for using solar modules alone as a low-cost alternative for estimating displacement and collecting context information indoors by measuring the radiant intensity (e.g. from overhead lighting). We expect that solar cells can be integrated into garments, e.g. on the user's shoulder. We present a theoretical model for ideal light sources without reflector and diffuser. We validate this model with experiments in an office corridor with evenly spaced fluorescent tubes using a trolley equipped with solar cells. Using a trained model, we estimate displacement with an error of 21 cm (confidence 80%) on straight trajectories using the data from a single solar cell. In order to determine the impact of user movement on the positioning accuracy, we then report experimental results of a user on a treadmill under fixed lighting. We show that light intensity varies significantly more with the horizontal displacement related to walking than the cyclic motion of the shoulder.

Single technologies have the strategic disadvantages that if the sensor system fails, is locally unavailable or suffers from drift (e.g. due to dead reckoning) the positioning service may fail or be unreliable. This supports the case for using multiple technologies. Since LuxTrace is a relative positioning approach based on tracking of individual lights the combination with an absolute positioning reference can be advantageous. We present a first concept to learn new lighting environments online by using an absolute position information when it is available. Applications may include corridor intersections where lighting conditions change or areas with mixed daylight and electrical light, e.g. in large rooms with multiple light sources.

Other investigations that have combined two technologies include the work of Lee et al. [10] and Randell and Muller [11]. However, these combinations are non-redundant, i.e. these systems require data from both sensors simultaneously. The HeyWow project [12] presented the idea of combining sensing technologies in parallel, i.e. with redundancy. Similar approaches with sensor fusion technology to ensure availability and to increase accuracy have been made in [13]. Angermann et al. [14] suggest that sensor measurements can be considered as a probability distribution function. Generalisations of sensor fusion technology have been presented in the COMPASS project [15] and in the Location Stack project [16].

We have selected RFID tags distributed in carpet-like foils on the floor as complementary technology since this technology offers an absolute reference positioning service with low-maintenance and low cost [17]. Moreover the memory capacity of the RFID tags could be used for providing additional location-dependent information in situ. We conducted initial experiments to study the combined system with a similar trolley and corridor to maintain comparability with the original experiments. The combined system collects location-dependent information from the RFID tags. Apart from online processing of position estimates, the combined system dynamically adapts to changes in the installed overhead lighting by means of an online model learning procedure. The results of the combined system indicate that a similar performance can be maintained in a more practical setting. Hence, the model learning approach is a feasible strategy for displacement estimation.

The paper follows the structure of our investigations. Firstly, we present our sensing approach and discuss issues related to it (Sect. 2). In Sect. 3 a general light emitter model for indoor light tracking is developed and evaluated. Section 4 presents our displacement estimation experiments and results. In Sect. 5 we present the initial experiments and results for the combined system. These results are assessed in the Discussion (Sect. 6). Finally we indicate further research directions in Sect. 7.

2 Solar cell navigation approach

In our sensing approach we use a solar module alone as a low-cost means to estimate displacement and collect context information indoors. We expect that solar cells can detect changes in the radiant intensity (e.g. from overhead lighting) when moved. Moreover this sensor can be easily integrated into garments, e.g. at the user's shoulder. Such modules can have similar characteristics to textiles e.g. low cost (~2 US), low weight (~20 g), low volume (~2 cm^3) and with a range of colours. A potential concept is shown in Fig. 1 in which the flexible solar module system on the shoulder (1), transmits one or more RF pulses only when there is sufficient energy to do so i.e. beneath a light source (2). This data is collected and processed on-body, e.g. by a belt worn computer (3) [18].

The environment is assumed to be static as the lights in the corridor are always on during office hours [19]. Whilst it is necessary to process the data from the solar modules, their relatively low bit rate is well adapted to on-body processing such as with a body worn computer.

We investigate how light data can be used to support indoor navigation systems. The issues relevant to LuxTrace

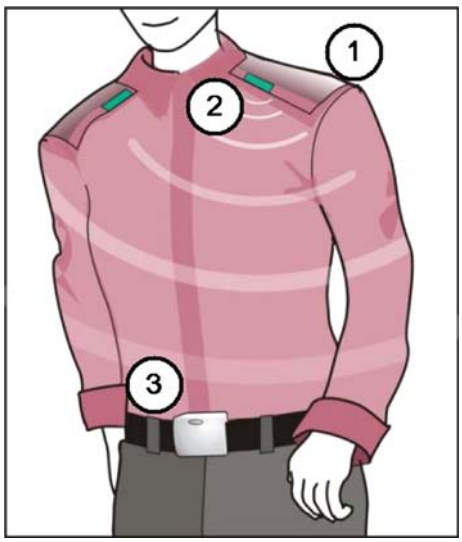

Fig. 1 LuxTrace concept: a wearable solar cells (*1*) attached to the user's shoulder, transmits measurements, e.g. via RF pulses (*2*) and on-body data processing, e.g. in a belt (*3*). Image by Ossevoort

can be categorised into three main areas: (1) the light sources providing the building illumination, that are used for tracking, (2) the environmental influences on the tracking of light sources and (3) the effects related to the user wearing the system. To demonstrate the scalability of our approach, we discuss in this section important items related to each area.

2.1 Light source related aspects

Distance and light angle: In an ideal case radiant intensity received at the solar cell declines at $1/r^2$ with increasing distance r between the solar cell and light source(s). Intensity is also reduced if the plane of the solar cell is not perpendicular to the incident light. This effect can support the light source tracking approach, since a maximisation of the voltage difference between ''peaks'' (maximum voltage) when the receiver is perpendicular under a light source and ''valleys'' (minimum voltage) when the receiver is between light sources is intended. The experimental conditions used in this work are outlined in Sect. 4.1 and a theoretical assessment is given in Sect. 3.

Light installation, diffusers and superposition: The way light sources are installed can affect measured radiant intensity. This can be related to the reflective and spectral properties of the objects around the light source such as diffusers and reflectors. Another aspect of light installation is encountered as the distance between two light sources is reduced: by superposition a light intensity maximum between two light sources can be created. Algorithms may misinterpret this intensity peak as a light source. Fortunately normal building lighting schemes avoid such pronounced superposition for energy efficiency and visual comfort reasons. Exceptions include areas where higher light level is required, e.g. work benches. Our experiments have been made with a standard diffuser type (see Sect. 4.1). Such pronounced superposition did not occur.

Types and power of lights: Light source intensity is related to the rated power (e.g. in the corridor tested the lighting tubes are rated 35 W whilst the adjoining offices are fitted with 58 W tubes). Manufacturers offer a wide range of light colours (e.g. Cool white) that might form a basis for distinguishing electrical light sources based on their different spectra.

Radiant intensity variances: Ageing effects of fluorescent tubes usually go unnoticed by the human eye, although an intensity reduction of ~20% can be expected in 2 years in an office environment. Intensity decrease can be exacerbated by dirt on the tubes, so that a loss of ~30% intensity in six months can be found in a garage for example.[1] The measurements made in Sect. 4 showed that the tubes tested had measurable (5%) differences in intensity. However, we do not anticipate that these differences would form a basis for identifying tubes that could be scaled up e.g. from a corridor to a building.

Light tube ballast identification: By modifying the fluorescent tube ballast, such lights have been used as a data broadcast channel. A number of scenarios can be found at [20]. Location tracking using fluorescent light sources might be simplified by having ballasts that allow each light to transmit a unique signature. A similar signature could be provided by LED lighting; this approach might provide wireless broadband (up to 1 GB/s) transmission capacity [21].

2.2 Issues Related to the Tracking Environment

Objects and wall reflection: Here we consider the influence of surroundings e.g. walls and objects. Their impact will depend on the distance to the objects from the light source(s), their shape and their reflectivity across the spectrum. Generally reflection contributes insignificantly to the overall indirect illumination [22]. Since this is a static property of a building section, it could be accounted for in building maps.

Availability of mapping information: It is understood that location systems that do not rely on such information being provided are generally preferred. Should map information be available, this information supports the tracking system by providing location constraints, e.g. impossible to walk through rigid objects such as walls. In

[1] Personal communication of the authors with a large Swiss light installation company.

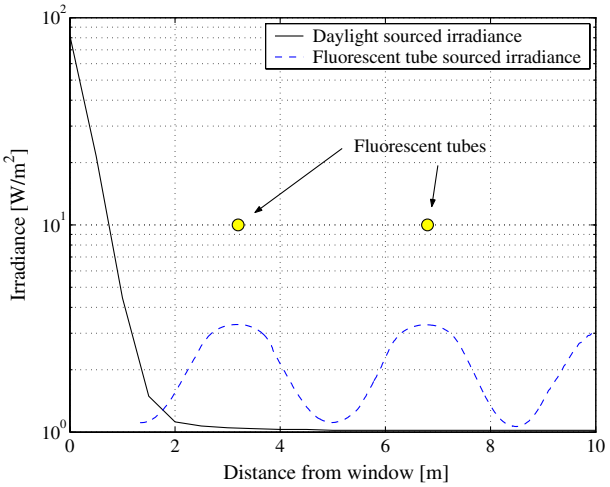

Fig. 2 Comparison of indoor irradiance source measurements, based on Fig. 3.28 in [22]

this work we assume the type and radiation intensity of the building lights is known for the system calibration.

Influence of natural light from windows: The tracking of artificial lights may be influenced significantly when solar cells are exposed to natural daylight near windows. However measurements showed that intensity of the natural light decays exponentially with the distance from the window and the window itself may have a transmissivity of 50% or less [22]. Hence at a distance of a few meters (depending on building and window form factor), the observed natural light intensity is lower than the indoor indirect light intensity[2] as shown in Fig. 2.

In all light tracking experiments direct natural light was avoided by simply keeping at least 3 m away from windows. However the windows could become a data source for tracking. In a case with daylight and artificial light from fluorescent sources only, e.g. an office building, natural light might be distinguished as it does not have the characteristic frequency variation (e.g. 100 Hz in Europe).

2.3 User related influences

Body constitution: Each user has a different physical constitution and body height which affects the distance to overhead lights. These differences lead to small offsets in the solar cell voltage as indicated in Sect. 3.

Movement: As the user moves, the position of the solar cells with respect to the body centre of mass will change e.g. due to user gait. Initial investigations of gait influence are made in Sect. 4.

[2] This assumes that direct light is partially transmitted or filtered by the window.

Shadowing effects: The head and/or the body can block light paths, reducing the intensity measured at the solar cell. Hence, we propose the shoulders as the primary place for mounting solar cells as these positions tend to be least obscured.

Clothing influence: For the case of solar cells on the shoulder, the orientation of solar cells with respect to the horizontal plane can be affected by looseness of clothing. For the current work a rigid type of solar cells was used.

3 Light intensity analysis and simulation

3.1 Radiant intensity modelling

In this first theoretical approach, we rely on radiant intensity information extracted from artificial light sources only. More precisely, in this analysis we consider a hallway scenario equipped with regular fluorescent light tubes installed in the ceiling at 2.5 m distance from the floor.

Many emitters can be modelled as a point source at sufficient distance. In this section, we apply a point source to depict the principle properties of light sources. However, since we aim to investigate the radiant energy of a light tube at different distances the model of a single point source is not sufficient. Therefore the fluorescent light tube was approximated as a bounded concatenation of point sources (Sect. 3.3).

3.1.1 Light emitter model

The source of radiant energy (emitter) creates a field of radiant flux. The total received flux per area is called *radiant intensity* (in W/m^2).

As the distance between light source and photovoltaic solar cell (receiver) changes, so does the radiant intensity received at the cell (radiant intensity). Radiant intensity I_{RPS} at a distance r from a point source emitting radiant energy with intensity I_0 is related by the inverse square law [22]:

$$I_{\mathrm{RPS}} = \frac{c_t I_0}{r^2} \qquad \text{with } c_t = \text{const. and } I_0 = \text{const.} \tag{1}$$

For positioning in 3D space the coordinate system x, y, z shown in Fig. 3 will be used, with its origin at the centre of the light source $0(x_0, y_0, z_0)$.

In the particular case where a receiver is positioned on a plane with z_S = const. near to the light source, the radiant intensity is at maximum if $x_S = x_0$ and $y_S = y_0$. This can be described as the total planar radiant intensity I_{TPS}. In the general case, for the radiant intensity at the solar cell sensor I_{SPS} an arbitrary angle ϕ must be considered, with $-90° \leq$

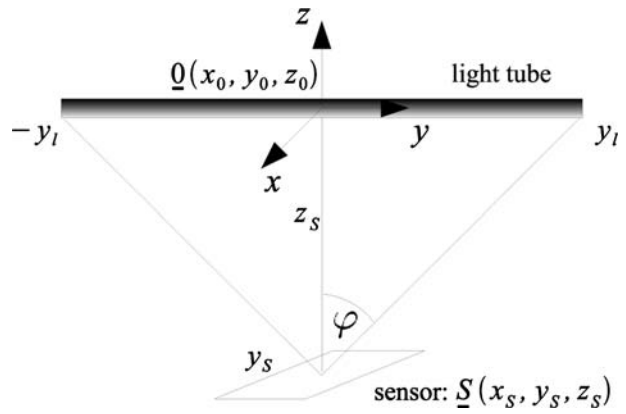

Fig. 3 Schematic for the light emitter model

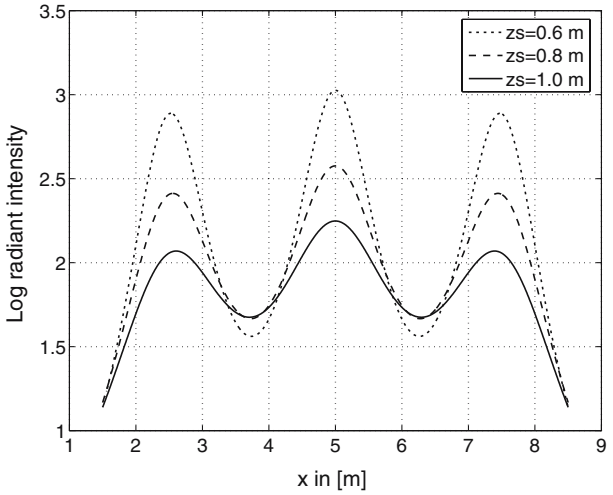

Fig. 4 Simulation of a movement along x under three point sources in 2.5 spacing at different ceiling distances z_S of S ($y_S = y_0$)

$\phi \leq 90°$ between the point source emitter and the receiving sensor, related by the cosine law: $I_{SPS}(\phi) = I_{RPS}\cos(\phi)$.

The distance r can be decomposed in the coordinate system by the three coordinates positioning the solar cell $S(x_S, y_S, z_S)$ (see Fig. 3) depending on the position along the light tube (y-coordinate).

$$r(y) = \sqrt{x_S^2 + (y_S - y)^2 + z_S^2} \tag{2}$$

In this representation ϕ is absorbed into $r(y)$. The radiant intensity from a point source I_{SPS} can be directly related to the coordinate system:

$$I_{SPS}(y) = \frac{cI_0 z_S}{(x_S^2 + (y_S - y)^2 + z_S)^{3/2}} \tag{3}$$

This relation can be used to simulate the radiant intensity received by a horizontal solar cell moving in any direction under light sources at arbitrary heights. The total radiant intensity I_S for a fluorescent light tube is found by approximating the light as a chain of point sources in y-direction:

$$I_S = \int_{-y_L}^{y_L} I_{SPS}\mathrm{d}y = \int_{-y_L}^{y_L} \frac{cI_0 z_S}{(x_S^2 + (y_S - y)^2 + z_S)^{3/2}}\mathrm{d}y \tag{4}$$

For simulations the distance to the light source, e.g. z-component z_S of S can be assumed to be constant. From the perspective in x-direction, the model assumes the light tube as a point source. Hence, x_S is constant. The total length of the light tube is denoted by l. Hence, the integration limits are described by $y_L = l/2$.

3.2 Detection of light emitters

The change in radiant intensity when varying the distance of a photovoltaic solar cell to the light emitter can be monitored by current or voltage variation. Whilst current is directly proportional to radiant intensity, voltage varies with the log of intensity: $V \propto \ln(I_S)$. For the simulation, the estimates $c = 1$ and $I_0 = 5$ W/m^2 were used. These values are fitted with real measurements to reflect size and type of the solar cells in the model.

Figure 4 shows the expected waveform for a straight trajectory equidistant to the walls down a corridor. The light tubes are oriented at right angles to the trajectory and regularly distributed. Since for this simulation example the y-component of the movement is $\Delta y = 0$, the light tubes are approximated as point sources. Assuming a typical office building height of about 2.5 m the distance z_S from an adult shoulder to the ceiling mounted light sources will be about 1 m or less. The regular distance d_L between the light tubes is greater than 2.5 m. Using the light emitter model a lower bound on the amplitude fluctuation can be derived: for the case of $d_L = 2.5$ m and $z_S = 0.8$ m there is a difference of 20% in the radiant intensity from the minimum to maximum value. This difference is deemed sufficient to correctly detect when the solar module is beneath a tube.

3.2.1 Environment effects and emitter model limitations

The light emitter model does not consider indirect light, such as reflections from walls and cupboards. As indicated in Sect. 2 indirect light generally has an order of magnitude less intensity than direct light, so this component of radiant energy has not been included in the light emitter model.

Occluded direct light can create distinct shadows hindering radiant energy reaching a sensor. For the intended application using overhead light sources, the possible obstruction area is limited to objects in direct line of sight

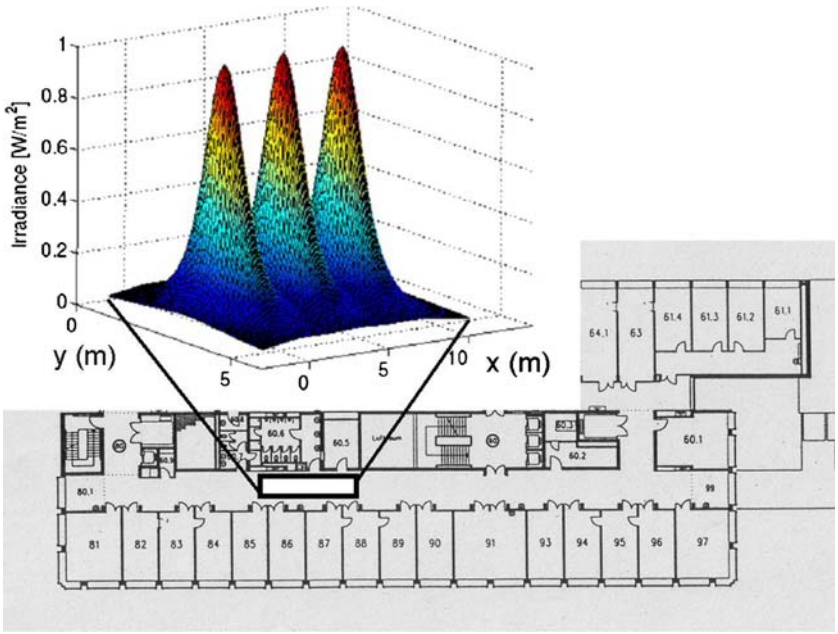

Fig. 5 Example of a simulated radiant intensity distribution as 3D plot for the scenario

with the light source, e.g. the box frame supporting the fluorescent light tube or the user's head. As this model does not cover human aspects in detail, the head is not considered.

3.2.2 *Light emitter based distance model*

In a second modelling step, a 3D environment for configurable light distributions was built for the majority of the corridors of our offices. With this approach it is possible to simulate various building scenarios. It is used here exclusively for a section of the corridor scenario.

For the following analysis of a hallway in an existing office building, the radiant energy distribution of fluorescent light tubes has been simulated as shown in Fig. 5. The simulation covers one long corridor leading to offices and a connecting passage. The simulated portion has three identical light tubes, equidistant with both walls, oriented in a perpendicular direction to the main corridor access. The distance between the lights is d_L = 3.7 m. There are no other significant sources of light in the scenario.

4 Light source tracking and activity estimation

4.1 Experiments

The initial goal of the experiments was to verify the waveforms calculated in the simulation. At the same time, measurement data were acquired for creating and validating an estimation model. This section details the measurement system used and the data sets acquired. Experiments were carried out within the corridor in which radiant energy had been simulated.

4.1.1 *Sensing system*

A measurement system based on a trolley was built that allows acquisition of the voltage from solar cells. The same set up was used for all experiments in this section. The solar module was positioned in a horizontal plane on top of the trolley. Furthermore, a relatively constant distance z_S between cell and fluorescent light tubes was maintained that varied by a few millimetres due to ground roughness under the wheels of the trolley for example.

The photovoltaic solar module used for the experiments is an amorphous silicon thin film deposited on glass.[3] The voltage of the solar cells was acquired at 1 kHz and 12 bit resolution using a standard data acquisition system. For convenience of signal acquisition, solar cell voltage across a 10 kΩ resistance was tracked in all experiments.

4.1.2 *Verification method*

To associate the acquired waveforms with actual distance down the corridor, two approaches were used: firstly we made measurements between manually located tags. This technique whilst relatively precise was limited in resolution since data could only be collected manually every ~50 cm.

Therefore a second distance measurement method was used: the front wheels of the trolley were replaced with bicycle wheels fitted with a standard bicycle dynamo. A

[3] Manufacturer: RWE SCHOTT Solar, model: ASI 3 Oi 04/057/050.

peak detection of the acquired voltage waveform from the dynamo generators was used to determine the system speed. The accuracy of the wheel measured distance compared to the distance determined by the first method was always over 98%. This accuracy was deemed sufficient and the second method was used to acquire ground truth for subsequent experiments.

4.1.3 Description of experiments

The experiments were performed pushing the trolley at constant walking speed (0.55 m/s) in an office corridor. A straight trajectory was taken below the middle of the light tubes. These tubes were integrated into the ceiling and oriented perpendicular to the walls of the corridor. The light diffusers were made of grooved (principle of Fresnel) colourless perspex. The distance between the horizontal solar cell and the fluorescent light tubes was $z_S = 73$ cm, the distance between the light tubes was $d_L = 3.7$ m.

The solar module voltage across the resistance of 10 kΩ was collected over trajectories of 2–10 m in length. Each time the solar module passed under a tube, a waveform peak was measured. A total of 14 such peaks were recorded.

Additional experiments were conducted to analyse if more detailed human motion than horizontal translation could be detected using solar cells. The shoulder was selected for placing the solar cell as we believe that this body position would be optimal with respect to maximising energy collected by the solar cell as well as ensuring optimal recognition of overhead lighting. We sought to quantify the effect of human walking motion as this would be a perturbation of a garment based distance measuring system.

A healthy male subject (69 kg) with body height 1.82 m, was selected who wore a close fitting T-shirt with Velcro sewn on the shoulders. The solar module was fixed onto the left shoulder and an acceleration sensor[4] was attached to his back at waist level (centre of mass). The subject walked on a treadmill that was running at a fixed speed. The subject's speed was kept constant by maintaining a relatively fixed position on the treadmill. The solar cell was directly beneath a fluorescent tube, similar to those installed in the corridor experiments. The subjects position was also equidistant from the ends of the fluorescent tube. Once the subject was comfortable with the speed, the solar module and acceleration sensors were synchronised and monitored for 1 min. Data were collected at four speeds (0.28, 0.83, 1.39 and 2.78 m/s) of the treadmill.

[4] Manufacturer: XSens Technologies B.V., model: MT9B.

4.2 Results

4.2.1 Light emitter model validation

To validate the light emitter model we compared the simulation result with the measured waveforms of the hallway scenario. The light emitter model varied over the range of 0.4–3.3 V whilst the average of the measured values was in the range 0.1–2.7 V. The simulation error for ten peak waveforms was less than 0.35 V in 80% and 0.4 V in 90% of all measurements. Part of the error can be attributed to the emitter model being for a bare fluorescent light tube rather than the measured data which was for an installed light tube including a reflective backing and a front diffuser.

4.2.2 Displacement estimation from the solar cell

Distance information can be extracted from the amplitude of the waveform by using a mapping between voltage and known distance from training data. To build the model, training data sets were segmented into single peak waveforms and scaled to the known light to light distance of $d_L = 3.7$ m. This empirical model was used in a simple mapping function which relates observed voltages from the solar cell and the average displacement under the light source.

To improve the displacement estimation for measurement outliers during testing that were not covered by the trained model, the last available speed information obtained with the same model was used. The average position estimation error (APEE) obtained with this method is less than 21 cm with a confidence of 80% over a distance of 7.4 m. The absolute position estimation error is depicted in Fig. 6.

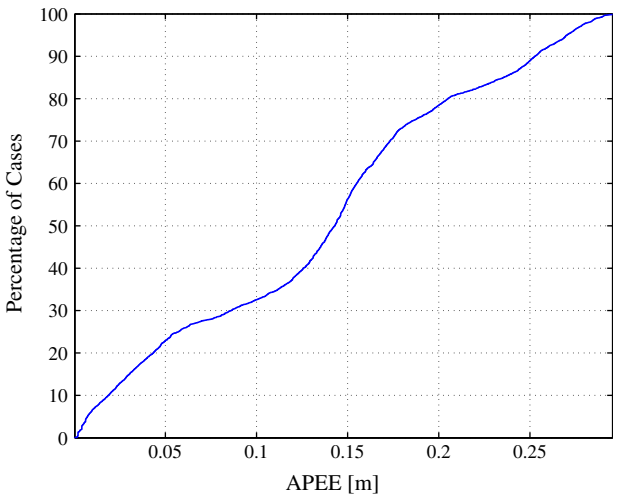

Fig. 6 Absolute position estimation error (APEE) of the empirical model

4.2.3 Human activity recognition

The vertical displacement of the human shoulder during locomotion is less than 10 cm. A point on the human shoulder makes a movement while walking that resembles a U shape when viewed from the front. This is the case for speeds from 1.6 to 2.3 m/s [23]. This displacement can be modelled by an overlay of harmonic sinusoidal functions.

A direct relationship in frequency and phase between the acceleration in the z-axis (up and down movement) and the solar module voltage was observed. We deduce that the cyclical trace at the solar cell is related to the striding motion of the subject [24]. Good correlations are achieved at treadmill speeds of 1.39 m/s and below. At higher speeds (e.g. when the subject is running), the estimation method incurred large errors and outliers. Furthermore, the walking waveforms showed some outliers for higher speeds that could be explained by abnormalities in the rhythmic movements, e.g. small jumps or bends of the torso. The peak to peak voltage variation induced by walking is low, e.g. 0.03 V at 1.39 m/s, suggesting satisfactory position tracking while walking can be expected as outliers are automatically ignored by the empirical model described above. Since walking introduced a low cell voltage variation, a low influence of walking on the position estimation by light tubes can be expected since outliers are automatically ignored by the empirical model described above.

Whilst a sinusoidal model resembles the solar cell measured trace, it is not a conclusive match, since the model does not include rotational (forward and back motion and swing) of the shoulder.

5 Extension of Lux Trace with absolute positioning information

We present our initial results on the extension of the LuxTrace system with absolute positioning systems. The motivation behind this investigation were twofold: (1) we evaluate an automatic online learning and integration strategy with absolute positioning systems and (2) we intended to gather more evaluation data.

5.1 System combination approach

The obvious motivation for combining positioning systems is reliability. A single system may fail or be locally unavailable for various reasons, see the issues related to the LuxTrace approach in Sect. 2. Another important feature is adaptability. The combination of well-selected position sensing methods can facilitate the system's adaptability to the current location. For LuxTrace this can be helpful, e.g. in interconnected buildings with different lighting schemes.

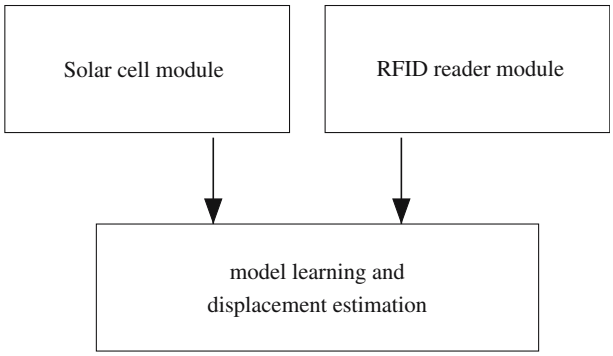

Fig. 7 Modules and signal flow in combined system

To evaluate the adaptability concept we use an online procedure for learning LuxTrace models with the help of additional absolute positioning information. The absolute positioning reference used in this work are carpet-like RFID foils distributed on the floor. These foils provide positioning information by the unique identification integrated in the tags that can be read when passing over them. The combined system consists of three parts: (1) the LuxTrace solar cell, (2) the RFID reading system and (3) the model learning and displacement estimation module. Figure 7 depicts the system architecture of the combined approach. The solar cell and RFID reading parts acquire sensed data; the model learning and estimation module is used for training and displacement estimation. The training of a LuxTrace displacement model is initiated whenever sufficient RFID readings are available. In this work we used the observation of one light period for the training, hence the RFID service must be available for individual lights only. The trained model is used immediately for the estimation. With this approach a sparse RFID distribution is possible, supporting the estimation of the solar cell at critical locations.

We selected RFID tags integrated in carpet-like foils as complementary technology for a number of reasons. Firstly, RFID technology offers an absolute reference positioning service with low-maintenance. Secondly, RFID is an inexpensive technology that is widely used. Thirdly, we could use the memory capacity of the RFID tags for providing additional location-dependent information in situ.

5.2 Experiments

5.2.1 Sensing system

The sensor hardware and the A/D converter experiments are the same as those used during the original LuxTrace experiments.

We have used an existing RFID positioning system developed at ETH Zurich as the absolute positioning ser-

vice [17]. It consists of two major components: (1) a trolley equipped with an off-the-shelf RFID tag reader and an RFID antenna, that is mounted at the bottom of the vehicle and (2) a carpet-like RFID tag infrastructure [25] that provides a dense distribution of RFID tags across certain areas of the floor space. The basic operating principle of the RFID positioning service is as follows: tag position coordinates stored on individual RFID tags are read that are within antenna range. The current position is computed as the arithmetical mean of the individual position readings obtained.

The LuxTrace equipment was added to the RFID positioning trolley. The complete system is shown in Fig. 8. The RFID antenna was attached under the base, at 10 cm above the floor space. At this distance, the approximately square operating area of the RFID antenna was about 50 × 50 cm. RFID tagged foils with an average tag density of 39 tags/m^2 were deployed.

For our practical experiments we chose an office corridor of similar type as the one used for the LuxTrace series of experiments, with light tubes of identical type, arrangement, and light emitting characteristics. We installed four RFID-tagged foil templates along the length of the corridor. The layout of our experimental setup is shown in Fig. 9. The solar cell was mounted on the trolley at 93 cm from the ceiling of the office corridor.

5.2.2 *Description of experiments*

We limited the observation range during the model learning procedure to a single low–high–low cycle of light intensities, as it is desirable to minimise the length of the corridor needed for the training of new models.

The placement of the RFID templates was chosen in a way that allowed us to obtain RFID position information in the critical sections halfway between adjacent light tubes, that can be used to support detection of low points in the measured light intensity.

All practical experiments were performed by pushing the measuring trolley at a constant walking speed of ~0.34 m/s along the test track.

In order to assess the positioning errors of the combined system under realistic conditions, each trained model would ideally be validated by comparing its position estimates to the actual trajectory along the test track a number of times, exposing it to different light intensity trace for each pass. For practical reasons, we experimentally measured and recorded multiple light intensity data streams along the same

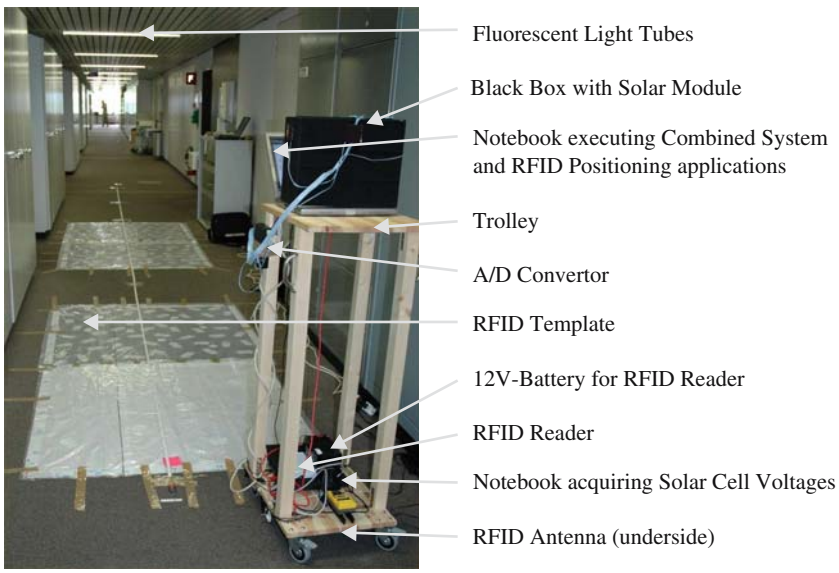

Fig. 8 Measurement trolley and prepared test track

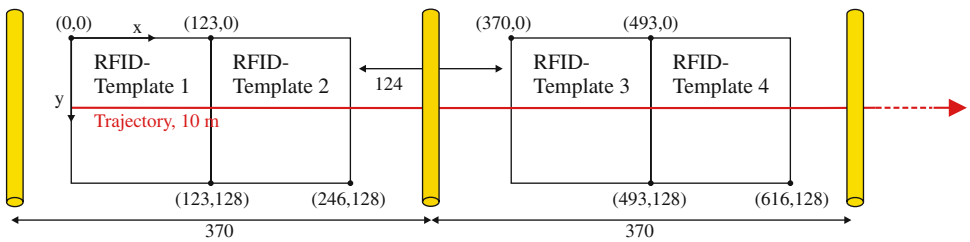

Fig. 9 Experimental setup: position of light tubes and RFID tagged foil templates (all coordinates and distances in cm). The test track starting at position (0, 60) is located at the start of the red arrow (trajectory 10 m)

trajectory. We then replayed these recorded experimental data streams in a simulation mode and compared them with the different recorded reference positioning data streams. We used this method to simulate further experiments and thus obtain additional data by cross-combining of data streams from different experiments.

5.3 Results

5.3.1 Displacement estimation of the combined system

We compared our results for the combined system with those previously reported in Sect. 4.

Figure 10 depicts the measured cumulative absolute positioning estimation errors (APEE) for the combined system and the original LuxTrace results for reference purposes.

Based on this plot, we can make the following observations: for the quantiles above 90%, the combined system has a significantly lower performance in comparison to the original LuxTrace result. However, for all quantiles ≤90%, the maximum error of the combined system never exceeds the maximum error of the LuxTrace reference system by more than 8 cm. For the 80 and 90% quantiles, the accuracy of the position estimates remain below 28 and 33 cm, respectively for the combined system, and below 21 and 25 cm, respectively for the original model. We consider these results an indication of the robustness of the online model learning approach, which merely relies on the analysis of a single light period in an arbitrary corridor. In contrast, the original LuxTrace model was trained with the data from 10 light period measurements for a particular corridor.

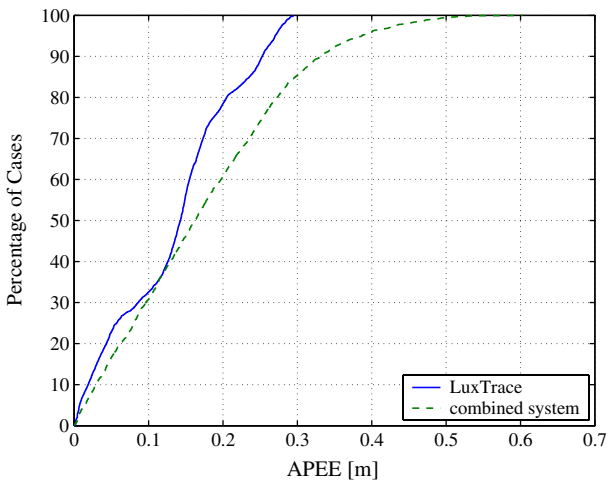

Fig. 10 Cumulative absolute positioning estimation errors of both investigated approaches: original LuxTrace model and combined system results

6 Discussion

We assess our results with respect to the location technology assessment taxonomy proposed by Hightower in the Location Stack project [26] that considers scalability, cost, recognition and limitations.

Scalability: A scalability factor related to cost is that as the solar cell devices and RFID tags are relatively cheap, it can be anticipated that the number of these devices, both solar cells on the body and RFID tags in the environment, should not be a limiting factor. For the solar cell based LuxTrace a wide application range in offices and manufacturing facilities is expected.

The combined system improves on the scalability of LuxTrace, as full coverage with both the solar cell and RFID systems is not required. Also, as RFID tags are fixed, they help to reduce the risk of drift from the solar cells.

Cost: For the LuxTrace system consisting of a solar cell and acquisition unit, a low cost implementation can be achieved. The global cost of the combined system includes incremental hardware, installation and maintenance. For a wearable device, we would anticipate that one or more antenna built into the shoe(s) would be used. This receiving device would be the highest power (Watt) incremental sensing device, and overall design would seek to minimise its duty cycle by switching when possible to the solar cell system (milliWatt) only. The corollary of such reduced power consumption is reduced mass, volume and cost for the battery; such components often have the highest values of the latter criteria in mobile systems.

A scenario minimising the installation cost of the RFID tags could be achieved if they were delivered as part of the carpet in a new building. Such tags could also be retrofitted under the existing carpet by using foils as used in the experiments of this work. A further way to minimise cost would be to install the tags only at intersections (e.g. corridor–corridor or corridor–room).

Further hardware costs are avoided as indoor lights and on-body computers (e.g. mobile phone) are generally available; incremental maintenance costs of the system would be minimal assuming that lighting infrastructure is not significantly changed and a bulb replacement service(s) exist.

Recognition: We have shown that recognition has not suffered despite the more practical scenario of the online model training and position estimation. Furthermore, combining the solar cell and RFID system improves reliability by supporting calibration of one system against the other. In this way our work presents a simple but robust feature fusion approach of the two systems. We manage the navigation system energy consumption and accuracy as follows: for maximum accuracy we can use both systems whilst for energy saving or for wearable computing sce-

narios, we selectively use only the lowest power (solar cell based estimator) system.

Limitations: The reported experiments focused exclusively on indoor applications in the absence of natural light. While this is sufficient for many room and corridor scenarios further work is necessary to determine the restrictions incurred from natural light sources.

7 Further work

Our experimental hardware is not adapted to wearable use and could be improved in a number of ways including, but not limited to, incorporating the RFID antenna into a pair of shoes, using flexible solar cells rather than glass deposited ones and experimenting with the use of multiple solar cells on the same user. Further experiments with humans would allow us to investigate more realistic scenarios, trajectories and location tracking durations.

In order to improve the wearability of the concept, the use of flexible solar cells (e.g. from [27]) would better match garment specification than those used in the experiments presented. Our results support the feasibility of future sensor nodes that rely on the same device for both sensing and energy harvesting.

Our models could also be improved with probabilistic algorithms, e.g. Kalman or particle filters. For the shoulder movement that we have investigated, a model based on rotations of a point on the shoulder in 3D space could be considered. Success in modelling such sources of context could also further support recognition accuracy.

It would be useful if LuxTrace could provide orientation around the vertical axis of horizontal solar cell. This might be inferred if the solar cells and light sources were equipped with polarising filters.

The combination of a low-power light sensing device (power requirements for A/D converter and voltage transformer: ~7 mW) with a relatively high power RFID system (power requirements: ~1 W) serves as an example of information fusion trade-off between coverage, accuracy and energy efficiency. The system could therefore adapt to maximum accuracy mode using the high-power RFID positioning system; an energy saving (wearable) mode would selectively use only the low power system. For maximum availability and coverage, both systems would be used in parallel.

8 Conclusion

We presented a concept to support location tracking with solar cells for indoor wearable applications. In our approach radiant energy from indoor building illumination is monitored by solar cells to derive displacement and context information.

After theoretical evaluation we presented experimental results indicating that a displacement estimation accuracy of 21 cm (80% quantile) can be achieved on straight trajectories. Additionally we evaluated the influence of human walking on the solar cell received irradiance.

In the second step we briefly investigated the collaboration of our system with an absolute positioning system. We developed a combined system consisting of a displacement estimator based on light sensing and information collected from carpet-like RFID tags distributed in the environment. The displacement estimator learns new lighting schemes online if RFID data is available. We found that the accuracy of the combined systems was similar (28 cm for 80% of all measurements).

We conclude that for the controlled conditions in which we experimented, LuxTrace (i.e. solar cells alone) are generally sufficient. An example application would be a linear displacement measurement on a track. However, for location tracking applications with less prior knowledge (e.g. spacing of lights, starting position, less predictable trajectories) the combined system may prove more accurate.

References

1. Getting I (1993) The Global Positioning System. IEEE Spect 30(12):36–47
2. Bretz EA (2003) Precision navigation in European skies. IEEE Spect 40:16
3. European Commission: (2005) Galileo project webpage. http://www.europa.eu.int/comm/dgs/energy_transport/galileo/index_en.htm
4. European Commission: (2003) The Galilei Project: GALILEO design consolidation. http://europa.eu.int/comm/dgs/energy_transport/galileo/doc/
5. Ni LM, Liu Y, Lau YC, Patil AP (2004) LANDMARC: indoor location sensing using active RFID. Wirel Netw 10:701–710
6. Vossiek M, Wiebking L, Gulden P, Weighardt J, Hoffmann C (2003) Wireless local positioning—concepts, solutions, applications. In: Radio and wireless conference. RAWCON '03.
7. Agiwal A, Khandpur P, Saran H (2004) LOCATOR: location estimation system For wireless LANs. In: WMASH '04: Proceedings of the 2nd ACM international workshop on Wireless mobile applications and services on WLAN hotspots, ACM Press, New York, 102–109
8. Andy W, Alan J, Andy H (1997) A new location technique for the active office. IEEE Pers Comm 4:42–47
9. Vildjiounaite E, Malm E, Kaartinen J, Alahuhta P (2002) Location estimation indoors by means of small computing power devices, accelerometers, magnetic sensors, and map knowledge. In: Pervasive '02: proceedings of the 1st international conference on pervasive computing, Springer, Berlin Heidelberg New York 211–224
10. Lee S, Mase K (2001) A personal indoor navigation system using wearable sensors. In: Proceedings of the 2nd international symposium of mixed reality (ISMR01), Yokohama

11. Randell C, Muller H (2001) Low cost indoor positioning system. In: Abowd GD Springer, Berlin Heidelberg New York 42–48
12. HeyWow Project: HeyWow project webpage (2005) http://www.heywow.com.
13. Bohn, J, Vogt H (2003) Robust probabilistic positioning based on high-level sensor-fusion and map knowledge. Technical Report 421, Institute for pervasive computing, Dept. of computer science, ETH Zurich
14. Angermann M, Kammann J, Robertson P, Steingass, A, Strang T (2001) Software representation for heterogeneous location data sources within a probabilistic framework. In: International symposium on location based services for cellular users (Locellus) 107–118
15. Kargl F, Bernauer A (2005) The COMPASS location system, LoCA, pp 105–112
16. Hightower J, Brumitt B, Borriello G (2002) The location stack: a layered model for location in ubiquitous computing. In: Proceedings of the 4th IEEE Workshop on Mobile Computing Systems & Applications (WMCSA 2002), Callicoon, IEEE Computer Society Press, New York, 22–28
17. Bohn, J (2006) Prototypical implementation of location-aware services based on super-distributed RFID tags. In: Proceedings of the 19th international conference on architecture of computing systems (ARCS'06), Frankfurt am Main, Germany. Number 3894 in LNCS, Springer, Berlin Heidelberg New York 69–83
18. Amft O, Lauffer M, Ossevoort S, Macaluso F, Lukowicz P, Tröster G (2004) Design of the QBIC wearable computing platform. In: Proceedings of the 15th IEEE international conference on application-specific systems, architectures and processors
19. Fox, D (1998) Markov localization: a probabilistic framework for mobile robot localization and navigation. PhD thesis, Institute of Computer Science, TU Dreseden
20. Talking Lights, Boston (2005) http://www.talking-lights.com/how.htm
21. Kavehrad M, Amirshahi, P (2005) Hybrid MV-LV Power lines and white light emitting diodes for triple-play broadband access communications. In: IEC comprehensive report on achieving the triple play: technologies and business models for success, ISBN: 978-1-931695-37-4. IEC, 167–178
22. Randall, J (2005) Designing indoor solar products. John, New York ISBN 0-470-01661-2
23. Cappozzo A (1981) Analysis of the linear displacement of the head and trunk during walking at different speeds. J Biomech 14:411–425
24. Amft O, Randall J, Tröster G (2005) Towards LuxTrace: using solar cells to support human position tracking. In: Proceedings of 2nd International Forum on Applied Wearable Computing, Zürich,
25. Bohn J, Mattern, F (2004) Super-distributed RFID tag infrastructures. In: Proceedings of the 2nd European Symposium on Ambient Intelligence (EUSAI 2004), Eindhoven, The Netherlands. Number 3295 in LNCS, Springer, Berlin Heidelberg New York 1–12
26. Hightower J, Borriello G (2001) A survey and taxonomy of location systems for ubiquitous computing. IEEE Comput 34:57–66
27. VHF-Technologies SA: Yverdon-les-Bains Switzerland. http://www.flexcell.ch (2005)